Soft Tissues and Materials

JOURNAL OF biomaterials applications

Journal of Biomaterials Applications
2022, Vol. 36(6) 1111–1125

DOI: 10.1177/08853282211046119
journals.sagepub.com/home/jba
SAGE

Macrophages, the main marker in biocompatibility evaluation of new hydrogels after subcutaneous implantation in rats

Tijana Lužajić Božinovski[1], Vera Todorović[2], Ivan Milošević[1], Bogomir Bolka Prokić[3], Vladimir Gajdov[1], Katarina Nešović[4], Vesna Mišković-Stanković[4] and Danica Marković[1]

Abstract

Biocompatibility of materials is one of the most important conditions for their successful application in tissue regeneration and repair. Cell-surface interactions stimulate adhesion and activation of macrophages whose acquaintance can assist in designing novel biomaterials that promote favorable macrophage–biomaterial surface interactions for clinical application. This study is designed to determine the distribution and number of macrophages as a means of biocompatibility evaluation of two newly synthesized materials [silver/poly(vinyl alcohol) (Ag/PVA) and silver/poly(vinyl alcohol)/graphene (Ag/PVA/Gr) nanocomposite hydrogels] *in vivo*, with approval of the Ethics Committee of the Faculty of Veterinary Medicine, University of Belgrade. Macrophages and giant cells were analyzed in tissue sections stained by routine H&E and immunohistochemical methods ($CD68^+$). Statistical relevance was determined in the statistical software package SPSS 20 (IBM corp). The results of the study in terms of the number of giant cells localized around the implant showed that their number was highest on the seventh postoperative day (p.o.d.) in the group implanted with Ag/PVA hydrogels, and on the 30th p.o.d. in the group implanted with Ag/PVA/Gr. Interestingly, the number of macrophages measured in the capsular and pericapsular space was highest in the group implanted with the commercial Suprasorb© material. The increased macrophage number, registered around the Ag/PVA/Gr implant on 60th p.o.d. indicates that the addition of graphene can, in a specific way, modulate different biological responses of tissues in the process of wound healing, regeneration, and integration.

Keywords

Histology, *in vivo*, macrophages, rats, silver/poly(vinyl alcohol)graphene, skin

Introduction

In accordance with the standard ISO-10993-1, Annex A, for implanted materials,[1] it is mandatory to determine the physicochemical characteristics and cytotoxicity, and it is necessary in further proceedings to include testing of tissue sensitization, tissue irritation response, systemic acute toxicity, chronic toxicity, histocompatibility, genotoxicity, carcinogenicity, biodegradation, and more, depending on the purpose in clinical trials.[2] Creating new materials, whose number has greatly increased following technological advances,[3–6] requires new standards for biocompatibility testing.[7] In that sense, it is proposed to examine cytotoxicity on specific cell lines (*in vitro*).[8,9] Finally, the most important step is to evaluate the tissue response *in vivo*, after implanting biomaterials in various animal models (large differences exist between animal species) prior to clinical use in human or veterinary medicine.[10–16]

[1]Department of Histology and Embryology, University of Belgrade Faculty of Veterinary Medicine, Belgrade, Serbia
[2]Department of Histology and Embryology, School of Medicine of University of Zenica, Zenica, Bosnia and Herzegovina
[3]Department of Surgery, Orthopedy and Ophthalmology, Faculty of Veterinary Medicine, Belgrade, Serbia
[4]Department of Physical Chemistry and Electrochemistry, Faculty of Technology and Metallurgy, University of Belgrade, Belgrade, Serbia

Corresponding author:
Danica Markovic, Department of Histology and Embryology, University of Belgrade Faculty of Veterinary Medicine, Boul. Oslobodjenja 18, Belgrade 11000, Serbia.
Email: danica@vet.bg.ac.rs

The evaluations include the foreign body reaction (FBR), inflammation, encapsulation, and the accumulation of macrophages in the periimplant zone.[11,13,17,18] Evaluation of any new PVA biomaterials for wound dressing requires analysis of the tissue reaction to the implanted material.[5,19–23] The introduction of silver nanoparticles (AgNPs) into polymer hydrogels increases their antimicrobial activity,[14,24–29] while the incorporation of graphene (Gr) improves mechanical properties.[30–33] In our long-term research, newly synthesized and previously *in vitro* characterized AgNP-loaded PVA-based polymer hydrogels were used[10,34] and then their biocompatibility was proven *in vivo*.[11] The type of tissue response to biomaterials depends on the nature,[35] structure, size and form of the implanted biomaterials,[36] the tissue area of implantation, and period of observation after implantation.[11,14,37] The FBR is followed bylocal inflammatory tissue response provoked by both the surgical incision and the presence of the biomaterial in the body, after which wound regeneration processes and fibrous encapsulation of the implanted materials begin.[18,38,39] The FBR includes a complex cascade of space-depended, interconnected processes such as triggering signals (soluble mediators—growth factors, cytokines, chemokines, and matrix metalloproteinases and their inhibitors) followed by cellular activation, involving inflammatory cells, angiogenesis, extravasation, cell migration, phagocytosis, and changes that occur in the biomaterial itself.[40]

Neutrophils are one of the first inflammatory cells that arrive at the implant site[11] and they have a crucial role which is reflected in the production of chemokines which attract other inflammatory cells, including monocytes.[41] The presence of neutrophils is followed by the expression of monocyte attractant chemokines MCP1 and MIP1α that act as pro-inflammatory regulators and through mediation with other pro-inflammatory factors (IL6 and IFN-γ) promote macrophage activation and their phagocytic behavior.[42]

The macrophage is an indicator of increased host protection against foreign bodies, acting as a phagocyte, engulfs small particles of foreign substances. In the case of larger materials such as implants, macrophages cannot absorb them, so they fuse together and form foreign body giant cells (FBGC).[43] The formation of these giant cells is mediated by the IFN-γ-induced TIMP-1 expression that stimulates secretion of IL-1 which in turn stimulates IL-13 synthesis that drives macrophage fusion.[44] Degradable biomaterials can be absorbed by phagosomes, or degrade over time, with or without the involvement of FBGC. Macrophages' responses to, and interactions with biomaterials, are not entirely understood currently.[45] In order for the material–cell interface to act optimally, specific performance of the FBR is required.[42] The biomaterial should provide a biomimetic environment to ensure cell survival and directed cell migration to ensure that relevant cells migrate to and adhere to the implant.[41,46] Macrophages take part in tissue remodeling that directly impacts the tissue repair process.[47,48] Nanotechnology and biomaterial science can greatly contribute to the design of devices for specific clinical needs, and the introduction of Gr has been shown to have various applications in medicine.[37] For example, Gr or carbon nanotubes, owing to their specific properties, have enormous potential as wound dressing fillers.[49,50] Graphene has even been used for the synthesis antibacterial nanomaterials; however, the specific mechanistic aspects of its antibacterial activity are still generally unknown and debatable.[51] Therefore, there is absolutely a great need for *in vivo* studies and extensive testing for all new graphene-based biomaterials intended for medical practice, in order to investigate the connection of these implantable biomaterials with the cellular components of the tissue reaction.[11] The *in vivo* data should provide the necessary evidences and enable development of better technologies for developing novel and biocompatible devices for clinical use.[46,52]

Our investigation is focused on the main cellular marker of biocompatibility, the macrophage, and aims to determine macrophage number and distribution around the implanted material in the rats' subcutaneous tissue by using histomorphometrical and histological methods.

Material and methods

Two hydrogels—silver/poly(vinyl alcohol) (Ag/PVA) and silver/poly(vinyl alcohol)/graphene (Ag/PVA/Gr)—were synthesized according to our original procedure presented in detail in the next paragraph, aimed for wound dressing. The soft tissue response to deep subcutaneous implants of Ag/PVA and Ag/PVA/Gr was monitored and compared to the reaction to a commercial wound dressing based on calcium alginate (Suprasorb©, Lohmann& Rauscher GmbH & Co. KG, Neuwied, Germany).

Electrochemical synthesis and characterization methods of nanocomposite Ag/PVA and Ag/PVA/Gr hydrogels

Silver/poly(vinyl alcohol) and silver/poly(vinyl alcohol)/graphene hydrogels were synthesized according to a carefully designed procedure that has been described in detail in our previous publications.[10,12,33] Briefly, the PVA and PVA/Gr colloid dispersions were first prepared by dissolution of 10 wt.% PVA in hot distilled water (90°C), whereas 0.01 wt.% graphene was added after cooling to obtain PVA/Gr dispersion. The components were mixed for several cycles by using magnetic stirring and sonication, until complete homogeneity was achieved. Afterward, the colloid dispersions were poured onto sterile Petri dishes up to 2 mm height and subjected to freezing and thawing cycles (five

cycles consisting of 16 h at −18°C and 8 h at +4°C) to obtain cross-linked hydrogels that were later cut into small discs (5 mm diameter) using a custom-made cutting tool. Thus, obtained hydrogel discs were loaded with silver ion precursor by swelling in 0.25 mM $AgNO_3$ solution (supplemented with 0.1 M KNO_3 to improve ionic conductivity). After 48 h of swelling, the hydrogels were placed inside a custom-designed electrochemical cell between two platinum electrodes, and subjected to 90 V constant voltage for 4 min to achieve reduction of Ag^+ and generate AgNPs directly inside the polymer matrix (*in situ*). The schematic representation of the hydrogels' preparation and the **AgNPs electrochemical** synthesis is presented in Figure 1.

Characterizations. Field-emission scanning electron microscopy (FE-SEM) was employed in order to confirm the successful synthesis of AgNPs, and the imaging was carried out using LEO SUPRA 55 microscope (Carl Zeiss, Germany) operated at acceleration voltage of **20 kV**. UV-visible spectroscopy was performed using CARY 300 Bio spectrophotometer (Varian Medical Systems Inc., Palo Alto, CA, USA) in 200–800 nm wavelength range, and the resulting peaks at ≈400 nm also confirmed the generation of AgNPs in Ag/PVA and Ag/PVA/Gr hydrogel matrices.

Silver was released from Ag/PVA and Ag/PVA/Gr in a phosphate buffer (PB) solution containing 0.39 mM KH_2PO_4 and 0.61 mM K_2HPO_4, at 37°C for 28 days, during which the PB medium was periodically replaced, and the removed solutions were analyzed using atomic absorption spectrometer (AAS) PYU UNICAM SP9 (Philips, the Netherlands). The total silver content was measured by treating the hydrogels with 1:1 (v/v) HNO_3 until they were completely dissolved.

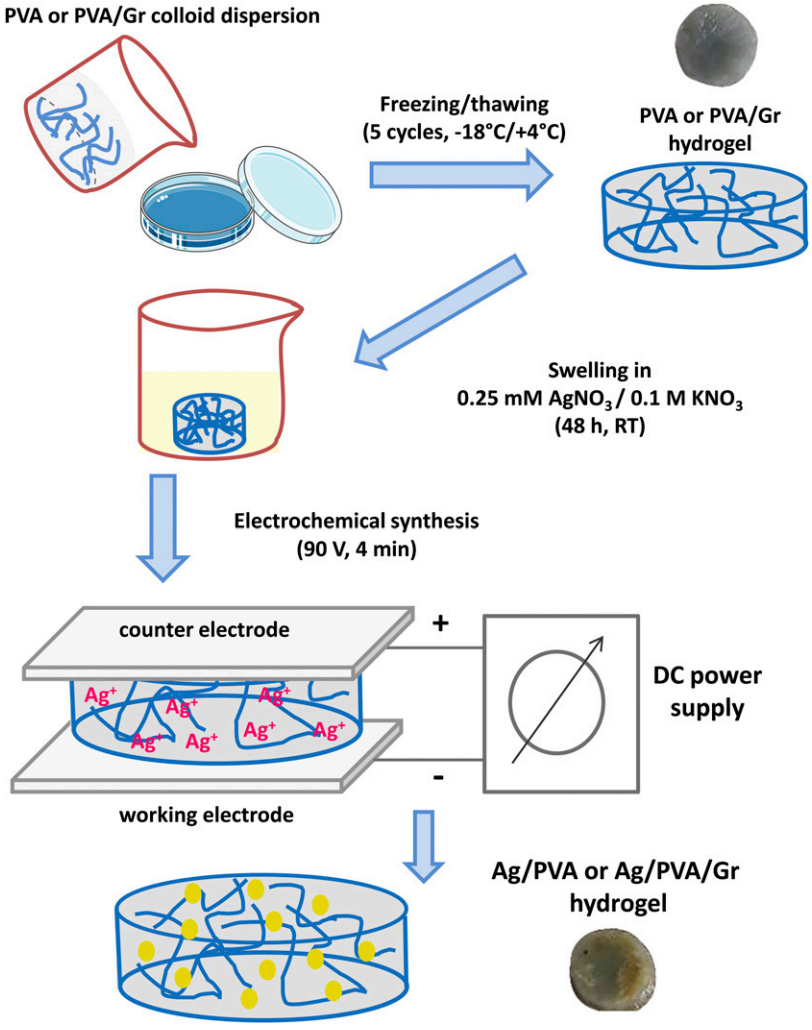

Figure 1. Schematic representation of the freezing/thawing cross linking and the electrochemical *in situ* synthesis of AgNPs inside Ag/PVA and Ag/PVA/Gr hydrogels.

The sorption characteristics of PVA, PVA/Gr, Ag/PVA, and Ag/PVA/Gr hydrogel discs were investigated by drying the hydrogels to a constant weight, and subsequently immersing them in simulated body fluid (SBF), as a model physiological medium, at 37°C, until equilibrium (constant weight) was reached. The swelling was monitored gravimetrically, by weighing the hydrogels at predetermined periods of immersion in SBF. The swelling ratios, q_t, were also calculated as the difference of the hydrogel mass at the defined time, m_t, and the mass of the dried gel before the experiment, m_0, divided by m_0 (equation (1)).

$$q_t(\%) = \frac{m_t - m_0}{m_0} \times 100 \quad (1)$$

The (3-(4,5-dimethylthiazol-2-yl)-2,5-diphenyltetrazolium bromide (MTT) assay was employed to evaluate the biocompatibility, that is, the cytotoxic effect of Ag/PVA and Ag/PVA/Gr hydrogels toward peripheral blood mononuclear cells (PBMCs) as well as the PBMCs that were stimulated to proliferation by phytohemagglutinin (PHA). The PBMCs were seeded in 24-well plates in nutrient medium, along with the samples of PVA, PVA/Gr, Ag/PVA, and Ag/PVA/Gr hydrogels, which were previously sterilized under **UV-C lamp**. The blank sample was a pure nutrient medium, whereas the cell suspension served as control. The second round of experiments was performed on proliferation-stimulated PBMCs. The entire experimental procedure was the same, except for the addition of mitogen PHA that was used to stimulate the PBMCs to proliferation. The cell viability was performed using the standard MTT assay, based on reduction of the yellow tetrazolium dye MTT to purple formazan inside viable cells' mitochondria. The cell survival rate was determined by measuring the absorbance at 570 nm using Multiskan EX Thermo Lab systems spectrophotometer (Thermo Scientific, USA), and viability was expressed as a percentage relative to the control.

The antibacterial activity was determined using two typical skin infection-inducing bacterial strains—*Staphylococcus aureus* TL (Gram positive) and *Escherichia coli* ATCC25922 (Gram negative) by standard broth-dilution test in suspension. Hydrogel discs were cut into ~1 mm^3 cubes and sterilized under UV-C lamp, after which they were immersed in a PB medium inoculated with bacterial cultures, and the number of bacteria after 1 h, 3 h, and 24 h of incubation at 37°C, using a colony counter. The number of viable bacterial cells was expressed as log (CFU mL^{-1}).

Experimental animals and hydrogel implantation procedure

Sixteen rats (Albino strain, Wistar breed), female, 3 months old, were used for subcutaneous implantation of the hydrogels, with the permission of the Ethics Committee of the Faculty of Veterinary Medicine, University of Belgrade. The materials used were as follows: Ag/PVA and Ag/PVA/Gr nanocomposite hydrogels prepared in the form of discs with a diameter of 5 mm and a thickness of 2 mm, as well as a commercial wound dressing based on calcium alginate, Suprasorb©. A small incision parallel to the spinal column was made and four pockets 0.5 cm in diameter were made deep in the subcutis into which the three appropriate implants were inserted. A fourth wound at the same distance and depth was made (pseudooperation zone) and it served for comparing the typical tissue reaction of an ordinary wound with the tissue reaction around the implant. All samples were controlled by observing the intact skin of the same animal, taken from the dorsal zone of the cervical region.

Surgical implantation technique

The implantation procedure was performed under general injection anesthesia, by intraperitoneal administration of 75 mg/kg ketamine hydrochloride (Ketamidor 10%, 100 mg/mL, RICHTER PHARMA AG, Austria) and 10 mg/kg xylazine (Xylased 2%, BIOVETA, Czech Republic). Prior to the procedure, butorphanol, 1 mg/kg (Nembutal, OAK) was administered subcutaneously for analgaesia. After the anesthesia, the operative site was shaved and disinfected with a solution of povidone-iodide. During preparation and operation procedure, the experimental animals were under constant monitoring by using a veterinary monitor (Votem v7 Patient-monitor, Korea). The animals were sacrificed by intraperitoneal injection of pentobarbitone solution, 160 mg/kg (Euthasol 400 mg/mL, Produlab BV, the Netherlands). After that, samples for histological analyses were taken from the implantation area, collected on the 7th, 15th, 30th, and 60th day after biomaterial implantation.

Preparation of histological specimens

The samples were prepared for histological analysis by routine procedure which included fixation in 4% neutral buffered formalin solution, followed by dehydration, clarification, impregnation, and paraffin/paraplast molding (Bio-Plast plus, BioOptica, Italy). Tissue samples were cut using a microtome (RM 2255, Leica Microsystems GmbH, Frankfurt, Germany). Tissue sections 4–5 μm thick were mounted on special glass plates coated with a strong adhesive (SuperFrost Plus, Dako, Germany), then stained with standard hematoxylin and eosin procedure (H&E). Macrophages and giant cells were counted around each implant, on 8–10 successive tissue sections stained with routine H&E and immunohistochemical methods ($CD68^+$) (Bio RAD, CA, USA, MCA34 1R).

The number of giant cells was expressed as the total number of cells localized in a 10 mm zone around the implant on each tissue section analyzed. Considering the variable size of giant cells around different implants, a semi-quantitative estimate was made as in what percentage of giant cells occupy the circumference of the ellipse, as follows: 0, no giant cells; 1+, up to 10% of the volume of the ellipse is occupied by giant cells; 2+, 11–30% of the volume of the ellipse is occupied by giant cells; 3+, 31–50% of the volume of the ellipse is occupied by giant cells; 4+, from 51 to 80% of the volume of the ellipse is occupied by giant cells; and 5+, over 80% of the volume of the ellipse is occupied by giant cells. All of these measurements were performed on a standard Olympus CX31 microscope and processed with the CellSens Entry morphometric measurement software (Olympus, Tokyo, Japan). Histological specimens were recorded with an Olympus UC50 digital camera.

Determination of macrophage abundance (CD 68 positive)

Macrophages stained with $CD68^+$ were marked in intact skin tissue and in periimplantation subcutaneous connective tissue around the biomaterials, as well as in the incision wound zone. The distinction among number of macrophages was performed in the capsule tissue formed around the hydrogel implant, as well as in the periimplant zone that directly bordered the capsule. Visualization of these markers was performed using a highly sensitive and specific two-stage indirect immunohistochemical technique using a dextran polymer to which secondary antibodies were directly bound in large numbers and which were labeled with radish peroxidase (Thermo Scientific UltraVision LP Detection System/HRP Chrome Polymer & DAB TL-060-HD, Lab Vision, USA). To visualize the antigen–antibody reaction, 3,3′-diaminobenzidine (Liquid DAB + Substrate Chromogen System, Dako, CA, USA) was used as a chromogen. Tissue sections were contrasted with Mayer's hematoxylin (Merck, Germany) and then mounted with a fitting medium (DPX). A commercial solvent was used to dissolve all the primary antisera (Dako Antibody diluent, S0809, Dako, Denmark), and 0.1 M PB pH 7.4 was used to wash the preparation between steps during the IHH staining procedure. The number of macrophages was determined in the dermis of the skin samples with implanted hydrogels, in the connective tissue capsule around the implant and in the subcutaneous connective tissue immediately surrounding the capsule (pericapsular zone) and expressed as the number of $CD68^+$ cells per mm^2 of surface area. Cells were counted in five representative areas of each sample. The measurement was performed with the Leica University Suite software system, version 4.3 (Leica Microsystems, Germany), on a Letz Labor Lux S Fluorescence Microscope (Ernst LeitzWetzlar GMBH, Germany). Histological specimens were recorded with a Leica DFC295 digital camera (Leica, Germany) (Figure 2).

Statistical processing of the results

From the data collected in the experimental research, a file was formed in the statistical software package SPSS 20 (IBM corp.) All results were expressed as mean ± SD. The minimum level of statistical significance was established at the level of $p < 0.05$. Descriptive and analytical statistics methods were applied. From descriptive statistical methods, measures of central tendency, and measures of variability were used, and from analytical statistical methods, analysis of variance for repeated measurements was used, within the general linear model. The results are presented in tables and graphs.

Results

Ag/PVA and Ag/PVA/Gr hydrogels characterization

The obtained Ag/PVA and Ag/PVA/Gr hydrogels with electrochemically synthesized AgNPs were fully characterized by different physicochemical and *in vitro* biological techniques, prior to the *in vivo* experiments. The successful AgNPs synthesis and incorporation was proven by FE-SEM. As can be seen from Figure 3, the AgNPs of approximately 20–50 nm are embedded in the polymer matrices. Using UV-visible spectroscopy, from the characteristic peaks at ≈408 nm for Ag/PVA and ≈405 nm for Ag/PVA/Gr) (data not shown) representing the surface plasmon resonance band of the AgNPs,[33] the AgNPs incorporation was additionally confirmed. These unique optical properties of AgNPs also caused the characteristic yellowish-brown color of the nanocomposite hydrogels (Figure 1).

The silver release behavior was monitored in modified phosphate buffered solution at 37°C using AAS and a characteristic "burst" effect was observed in the initial 3–5 days period, as shown in Table 1. The initial concentration of silver inside the hydrogel matrices was measured to be 41.3 ± 8.0 mg dm^{-3} in Ag/PVA and 28.2 ± 1.7 mg dm^{-3} in Ag/PVA/Gr, whereas it decreased to 27.1 ± 5.4 mg dm^{-3} and 18.5 ± 3.0 mg dm^{-3}, respectively, after 5 days of release. This burst release behavior is particularly important since it helps prevent adhesion of bacteria immediately upon wound dressing or soft tissue implant application. However, continuous silver release in the long-term (28 days) was also observed, as evidenced by the fact that only 13.3 ± 3.8 mg dm^{-3} and 9.7 ± 3.6 mg dm^{-3} remained in the Ag/PVA and Ag/PVA/Gr hydrogels, respectively, after 28 days (Table 1), confirming that up to 60–70% of the total silver concentration was released during

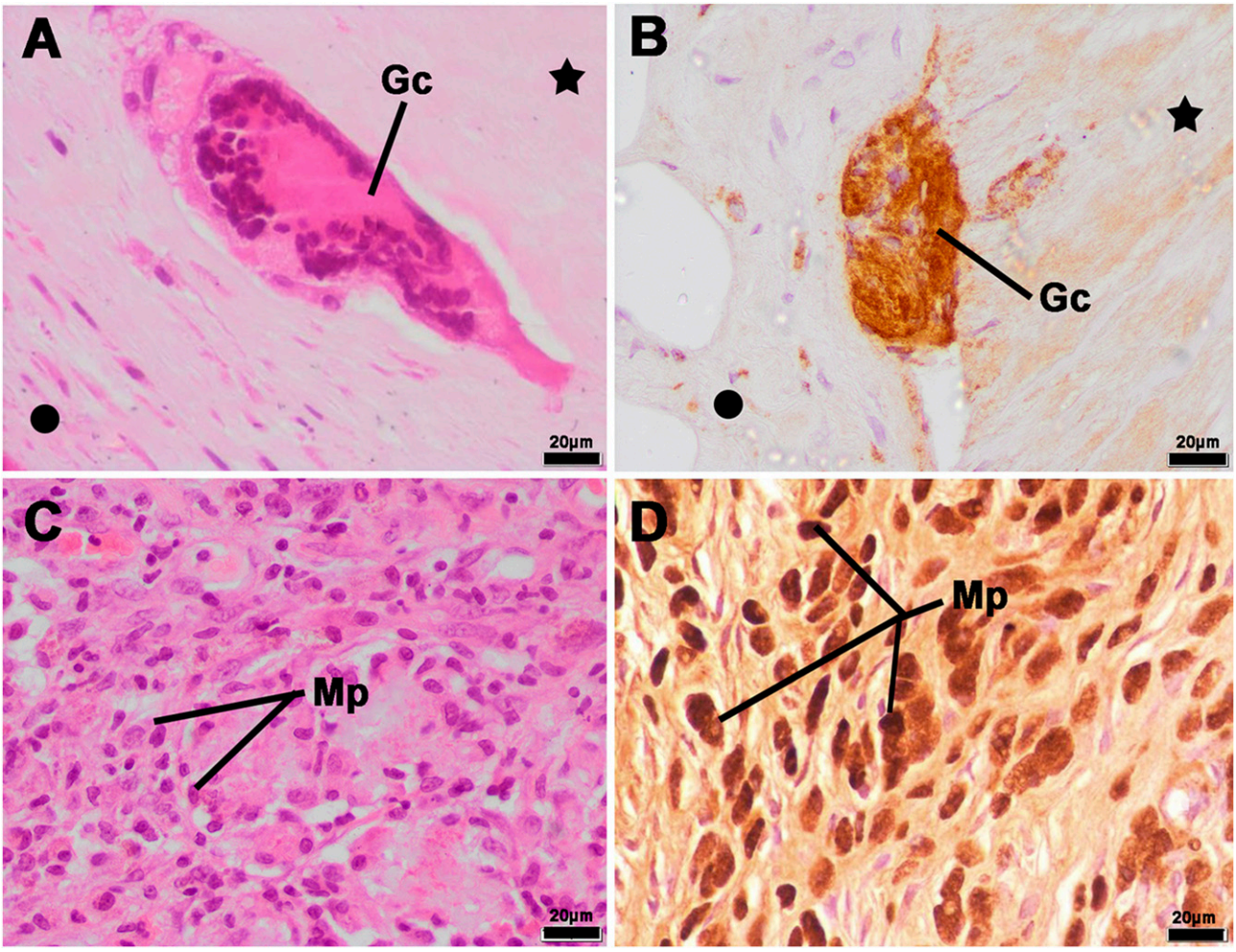

Figure 2. Giant cell and macrophage determination, (dot – capsule, Gc – giant cell, star – implant location, Mp - macrophage), H&E – a, c; Immunohistochemistry CD 68 – b, d; bar: 20 μm.

this observed period, which is undeniably desirable to prevent biofilm formation and preserve sterility over time.

Another quite important property for wound dressing hydrogel materials is their swelling ability, that is, their behavior during sorption of wound exudates. As described above, the swelling ability of PVA, PVA/Gr, Ag/PVA, and Ag/PVA/Gr hydrogels was investigated in SBF at 37°C. The obtained masses, m_t, and swelling ratios, q_t, are presented in Table 2 for all four types of hydrogels. The measured swelling ratios revealed that the hydrogels initially swell very quickly and reach almost two times their initial dry weight during the first 24 h ($q_t \approx 100\%$). Furthermore, the equilibrium swelling ratios reached after 72 h are between 200 and 300%, attesting to the excellent ability of these hydrogels to absorb and retain moisture, which is certainly beneficial for wound healing. It could also be observed from Table 2 that the equilibrium swelling ratios are lower for hydrogels loaded with AgNPs (≈228% and ≈212% for Ag/PVA and Ag/PVA/Gr, respectively), compared to pure PVA (≈233%) and PVA/Gr (≈261%), indicating that the presence of AgNPs contributes to the rigidity of the polymer matrix and slightly hinders swelling.

Furthermore, the *in vitro* biological assays were performed in order to assess the appropriateness of the synthesized nanocomposite hydrogels for intended applications. The cytotoxicity results confirmed good biocompatibility of the AgNP-loaded hydrogels, as the viability of both proliferating and non-proliferating cells remained always close to or above 70%, as shown in Table 3. According to a cytototoxicity scale,[53] the materials exhibiting cell viability of 60–90% could be classified as only mildly cytotoxic, confirming that the synthesized AgNP-loaded hydrogels are safe for biomedical use.

Based on the antibacterial activity investigations, the Ag/PVA and Ag/PVA/Gr hydrogels manifested potent and rapid antibacterial effect, completely eradicating *S. aureus* TL colonies after 3 h post-incubation and *E. coli* ATCC25922

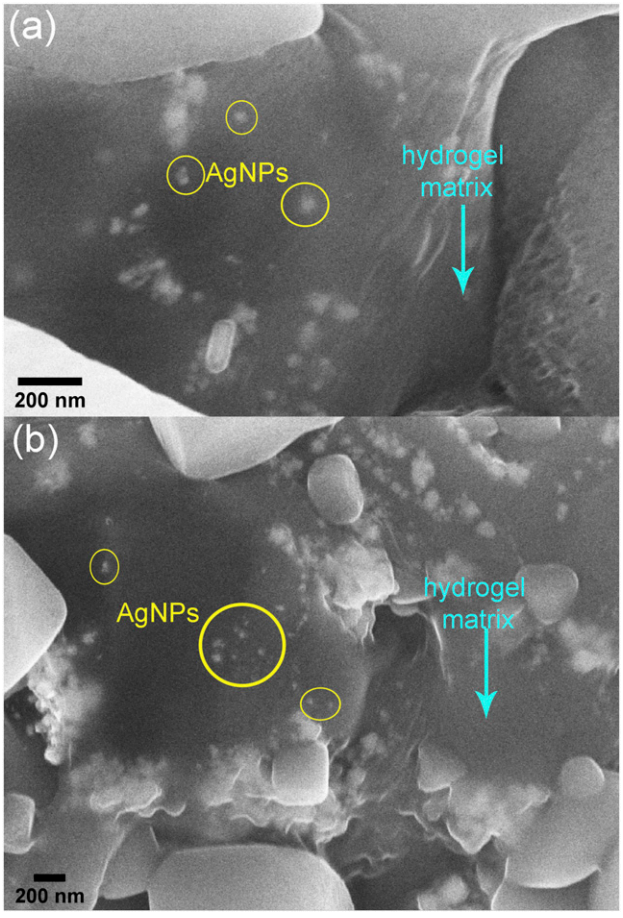

Figure 3. Field-emission scanning electron microscopy microphotographs of (a) Ag/PVA and (b) Ag/PVA/Gr hydrogels with marked representative silver nanoparticles and the surrounding polymer matrix.

after only 1 h incubation period (Figure 4). All these *in vitro* results pointed to significant potential of the nanocomposite Ag/PVA and Ag/PVA/Gr hydrogels for biomedical applications, especially for active antibacterial wound dressings or soft tissue implants, so the logical next step was in-depth examination of their *in vivo* responses in animal model.

Giant cells around the foreign body (different hydrogels implants) localized in the subcutaneous tissue

The presence of giant cells around the foreign body localized around the subcutaneously implanted hydrogels (Ag/PVA, Ag/PVA/Gr and Suprasorb©) during postoperative follow-up (day 7, day 15, day 30, and day 60) is shown in Figure 5(a). The results of the giant cells number study, localized around the implant, showed that the number of these cells was highest on the 7th p.o.d. in the group implanted with Ag/PVA and Suprasorb© (Figure 5(b), (c), (f) and (g)). With the

Table 1. The silver release profiles, presented as silver concentration remaining in the hydrogel, c_{Ag}, versus time of silver release, t, in the phosphate buffered solution at 37°C, for Ag/PVA and Ag/PVA/Gr hydrogels.

	0.25 Ag/PVA	0.25 Ag/PVA/Gr
t (day)	c_{Ag} (mg dm^{-3})	
0	41.3 ± 8.0	28.2 ± 1.7
1	33.6 ± 5.8	23.7 ± 2.1
2	30.8 ± 5.3	21.5 ± 2.8
3	29.4 ± 5.3	20.5 ± 2.9
4	28.2 ± 5.4	19.5 ± 3.0
5	27.1 ± 5.4	18.5 ± 3.0
6	25.9 ± 5.3	17.7 ± 3.1
7	24.3 ± 5.3	16.4 ± 3.1
12	21.7 ± 4.8	14.4 ± 3.6
16	19.3 ± 4.0	13.0 ± 3.3
21	16.7 ± 3.4	11.3 ± 3.2
28	13.3 ± 3.8	9.7 ± 3.6

new Ag/PVA/Gr material, a gradual increase of giant formations is observed from day 7 to day 30 when it reaches peak (Figure 5(a) and (d)). On the 60th p.o.d., the number of giant cells drops by 45% compared to day 30 (Figure 5(e)). In the group implanted with Ag/PVA, the periimplant connective tissue analysis showed that giant cells' number reached a peak on the seventh day p.o.d. and then declined, maintaining similar values on the 15th and 30th day p.o.d. and then statistically significantly decreasing on day 60th p.o.d. In the case of Suprasorb© preparation, the giant cell population numbers are highest on the 7th p.o.d. and successively and uniformly decrease toward day 60 p.o.d., although it should be noted that the total values in this category are three and four times lower compared to the values gained for the other biomaterials (Ag/PVA and Ag/PVA/Gr) (Table 4). In contrast, in the case of Ag/PVA/Gr implants, the number of giant cells increased linearly until the 30th p.o.d., to be significantly reduced on the 60th p.o.d. (Table 4 and Figure 5(a), (d) and (e)). However, the number of giant cells around Ag/PVA/Gr implants at the end of the follow-up period, on the 60th p.o.d., was significantly higher (9.9360 ± 1.9030) compared to the same number in Ag/PVA implantation (3.8835 ± 0.7822) and Suprasorb© (1.9030 ± 0.7054). Also, compared to Suprasorb©, the number of giant cells at the end of the follow-up period was higher in the case of Ag/PVA implant (Table 4).

Macrophages in the periimplant zone after subcutaneous application of silver/poly vinyl alcohol, silver/poly vinyl alcohol/graphene and suprasorb©

The number of macrophages in the connective tissue capsule and pericapsular connective tissue after subcutaneous implantation of the different hydrogels at different time periods during the postoperative monitoring period is shown in

Table 2. The swelling profiles, representing the time dependence of the hydrogel mass, m_t, as well as the swelling ratio, q_t, during swelling in the SBF medium at 37°C, for PVA, PVA/Gr, Ag/PVA and Ag/PVA/Gr hydrogels.

	PVA		PVA/Gr		Ag/PVA		Ag/PVA/Gr	
t (h)	m_t (g)	q_t (%)	m_t (g)	q_t (%)	m_t (g)	q_t (%)	m_t (g)	q_t (%)
0	0.0513	0.0	0.0510	0.0	0.0544	0.0	0.0661	0.0
1	0.1100	114.4	0.1017	99.4	0.0993	82.5	0.1146	73.4
2	0.1314	156.1	0.1239	142.9	0.1101	102.4	0.1422	115.1
3	0.1415	175.8	0.1405	175.5	0.1380	153.7	0.1477	123.4
4	0.1547	201.6	0.1442	182.7	0.1466	169.5	0.1640	148.1
5	0.1561	204.3	0.1576	209.0	0.1528	180.9	0.1703	157.6
6	0.1592	210.3	0.1599	213.5	0.1554	185.7	0.1816	174.7
7	0.1622	216.2	0.1616	216.9	0.1585	191.4	0.1887	185.5
8	0.1666	224.8	0.1676	228.6	0.1597	193.6	0.1911	189.1
9	0.1670	225.5	0.1725	238.2	0.1634	200.4	0.1918	190.2
10	0.1672	225.9	0.1746	242.4	0.1654	204.0	0.1922	190.8
11	0.1675	226.5	0.1765	246.1	0.1721	216.4	0.1927	191.5
12	0.1732	237.6	0.1784	249.8	0.1756	222.8	0.1964	197.1
24	0.1707	232.7	0.1846	262.0	0.1762	223.9	0.1977	199.1
36	0.1710	233.3	0.1848	262.4	0.1783	227.8	0.2014	204.7
48	0.1704	232.2	0.1844	261.6	0.1836	237.5	0.2065	212.4
60	0.1706	232.6	0.1845	261.8	0.1801	231.1	0.2061	211.8
72	0.1708	232.9	0.1841	261.0	0.1782	227.6	0.2060	211.6

Table 3. MTT cytotoxicity assay results for PVA, PVA/Gr, Ag/PVA and Ag/PVA/Gr hydrogels representing the cell viability data for non-proliferating PBMC cells as well as PBMC cells stimulated to proliferation by PHA.

Cell viability (%)		
Hydrogel	PBMC	PBMC + PHA
PVA	90.8 ± 0.9	84.0 ± 7.9
PVA/Gr	84.2 ± 6.7	72.7 ± 6.2
Ag/PVA	82.5 ± 5.4	75.6 ± 8.3
Ag/PVA/Gr	69.4 ± 15.3	68.0 ± 14.9

Ag/PVA: silver/poly(vinyl alcohol); Ag/PVA/Gr: silver/poly(vinyl alcohol)/graphene; PHA: phytohemagglutinin; PBMC: peripheral blood mononuclear cell.

(Figure 6(a) and (b)). High result values in both connective tissue categories around the Suprasorb© implant (capsular and pericapsular) were expected, considering the nature of the commercial calcium alginate material, which is easily decomposed in the extracellular matrix of the dermis (Figure 6(e), (h), (k) and (n)). The structure of the polyvinyl hydrogels enriched with silver and graphene particles stimulate capsule formation and collagenation, increasing leukocyte infiltration. Macrophages are present in all the periods and throughout all skin regeneration phases (Figure 6(c), (d), (f), (g), (i), (j), (l) and (m)). Differences in macrophage number at different time periods are in accordance with the expected tissue response to

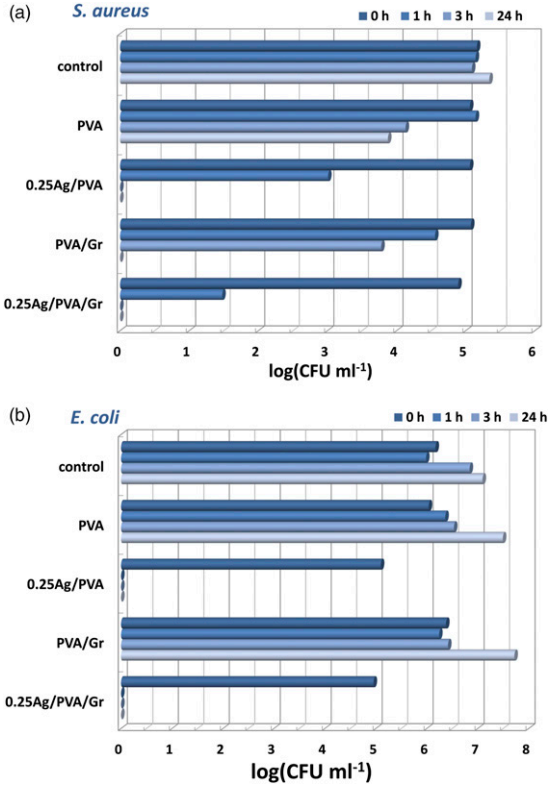

Figure 4. Antibacterial properties of PVA, PVA/Gr, Ag/PVA and Ag/PVA/Gr hydrogels against (a) *Staphylococcus aureus* TL and (b) *Escherichia coli* ATCC25922 bacterial strains.

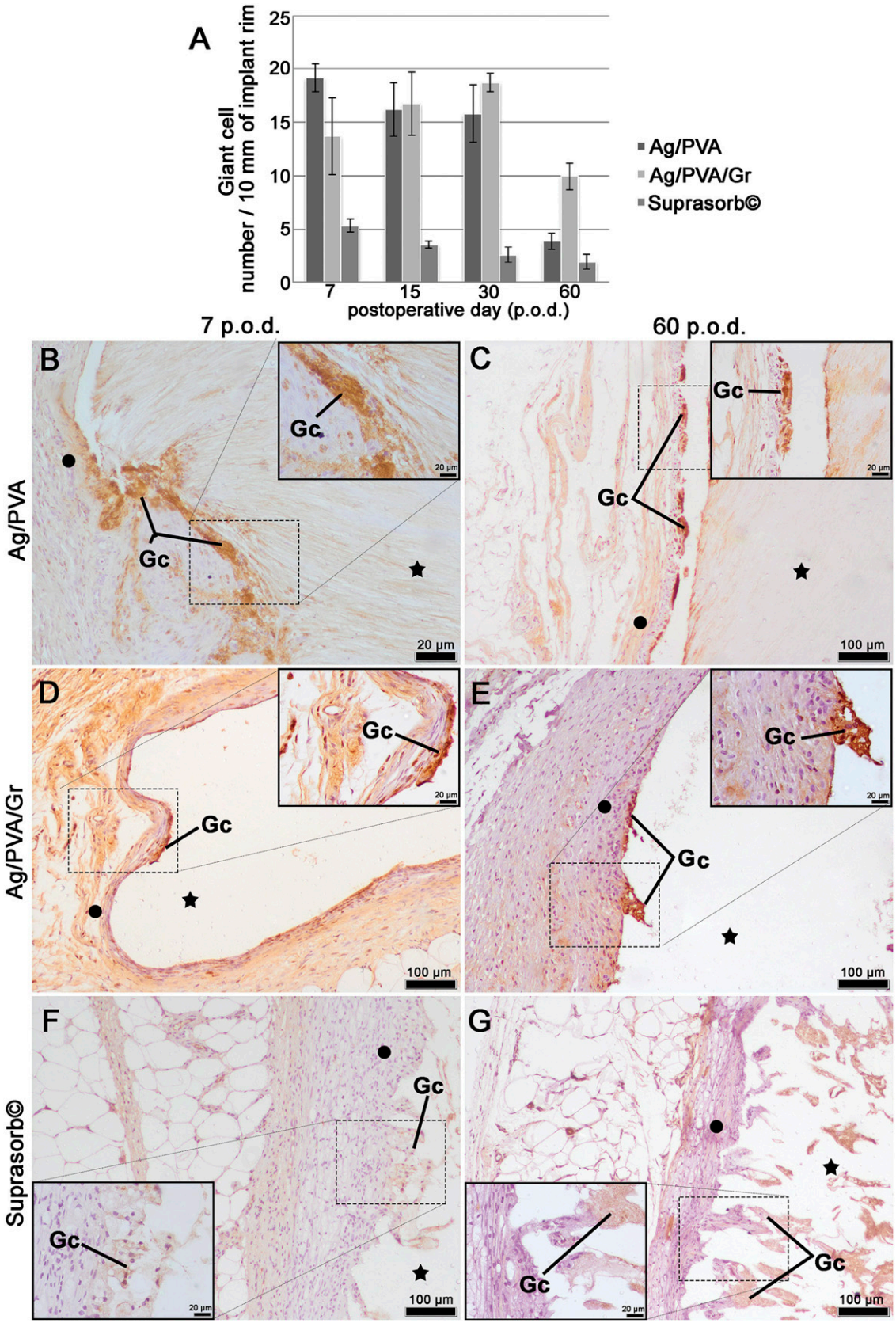

Figure 5. (a) Giant cells around the foreign body (dot – capsule, star – implant location, Gc – giant cells), Ag/PVA, 7th and 60th p.o.d. (b, c); Ag/PVA/Gr, seventh and sixtieth p.o.d. (d, e); Suprasorb©, 7th and 60th p.o.d. (f, g). Bar: 100 µm, black bordered frames represent area under high magnification – bar: 20 µm.

Table 4. Statistical representation of foreign body giant cells localized around the implanted hydrogels, 7th, 15th, 30th, and 60th postoperative day (p.o.d.).

Group		Ag/PVA	Ag/PVA/Gr	Suprasorb©
1	X (mean value, N/10 mm)	19.1690	13.7450	5.3375
	N	20	20	20
	SD (standard deviation)	1.35787	3.61349	0.59266
2	X (mean value, N/10 mm)	16.2535	16.7660	3.5040
	N	20	20	20
	SD (standard deviation)	2.50949	2.94098	0.34235
3	X (mean value, N/10 mm)	15.8070	18.7240	2.5880
	N	20	20	20
	SD (standard deviation)	2.70025	0.88310	0.68795
4	X (mean value, N/10 mm)	3.8835	9.9360	1.9030
	N	20	20	20
	SD (standard deviation)	0.78217	1.23831	0.70542

1: 7th (p.o.d.); 2: 15th (p.o.d.); 3: 30th (p.o.d.); 4: 60th (p.o.d.); Ag/PVA: silver/poly(vinyl alcohol); Ag/PVA/Gr: silver/poly(vinyl alcohol)/graphene.

the implanted materials. Thus, the increased number of macrophages in the periimplant connective tissue surrounding the Ag/PVA/Gr material, on the 15th p.o.d. is a part of the physiological skin healing process during the chronic stage of wound inflammation, followed by phagocytosis which is desirable tissue reaction to a foreign body (Figure 6(a), (b) and (g)).The number of macrophages in the capsule and pericapsular connective tissue in all observed periods was generally highest in the group implanted with Suprasorb©, in regard to the Ag/PVA and Ag/PVA/Gr implants (Figure 6(a) and (b)). The number of macrophages in the capsule and pericapsular zone was highest in the group implanted with Suprasorb© on the seventh p.o.d. compared to the other two hydrogels and decreased slightly during the follow-up period (Figure 6(e)). Furthermore, in all the groups, the capsule was more densely infiltrated by macrophages in relation to the pericapsular zone. In the group implanted with Ag/PVA, the macrophage infiltration density of the connective tissue capsule was initially lower on the 7th and on the 15th p.o.d. it gradually increased, so that macrophages on the 30th p.o.d. infiltrated the capsule in a similar manner as they did in the group implanted with Suprasorb©.However, such a trend did not continue in the 60th p.o.d. since the density of macrophages' infiltration of the capsule around Ag/PVA was significantly lower in the same time period in the group implanted with Suprasorb© (Figure 6 (l) and (n)). In the group implanted with Ag/PVA/Gr, the density of macrophage infiltration of the connective tissue capsule was significantly lower on the 30th p.o.d. compared to the infiltration of the capsule around Suprasorb© in the same period (Figure 6(j) and (k)). The capsule around Suprasorb© was not as clearly defined as the capsules around the other hydrogels, on the 7th, 15th, and 30th p.o.d.

Discussion

In one of our previous research studies, we used immunohistochemistry to analyze and visualize skin regenerative processes after subcutaneous implantation of Ag/PVA and novel Ag/PVA/Gr hydrogels in an animal model.[54] The biocompatibility markers' *in vivo* evaluation demonstrated tissue remodeling processes. We observed cellular and extracellular components such as laminins, vessel density and angiogenesis in the wound bed, collagenization, capsulation, fibroblast and keratinocyte migration, and proliferation on the 7th, 15th, 30th, and 60th p.o.d. In the present study we focused on macrophages as they are one of the most important cells in the FBR. We presented a comparative analysis of three different biomaterials, two of which have already been tested and have proven their safety *in vivo* (Ag/PVA and the commercial Suprasorb© implants) while the third material is new and untested and was synthesized using advanced nanotechnology methods Screening tests deal with results comparison of semi-quantitative data and morphometric and immunohistochemical methods which adhere to the criteria prescribed by the standards used in the assessment of the Tissue Irritation Index (TIRI), that is, the degree of tissue damage. In our study, it was reported that the tissue response parameters, tissue damage degree, and duration of tissue recovery around the implant are significantly statistically lower comparing to the tissue inflammatory reaction at the surgical incision site (pseudooperation).[11,13] Macrophages are the basic parameter of these tissue changes, and their number rises in the chronic phases of the wound healing process.[55] Collagenation, encapsulation, and magnification of tissue macrophages are indicators of a receding tissue reaction and its gradual recovery and healing.[54,56] The renewal of the matrix components (collagen), the restraint of the foreign body by encapsulation, and the increase in macrophages and giant cells number are an indicator of normal tissue defect regeneration.[43,48] Thus, an increase in the number of macrophages on the 15th and 30th day in our observation is an indicator of low to

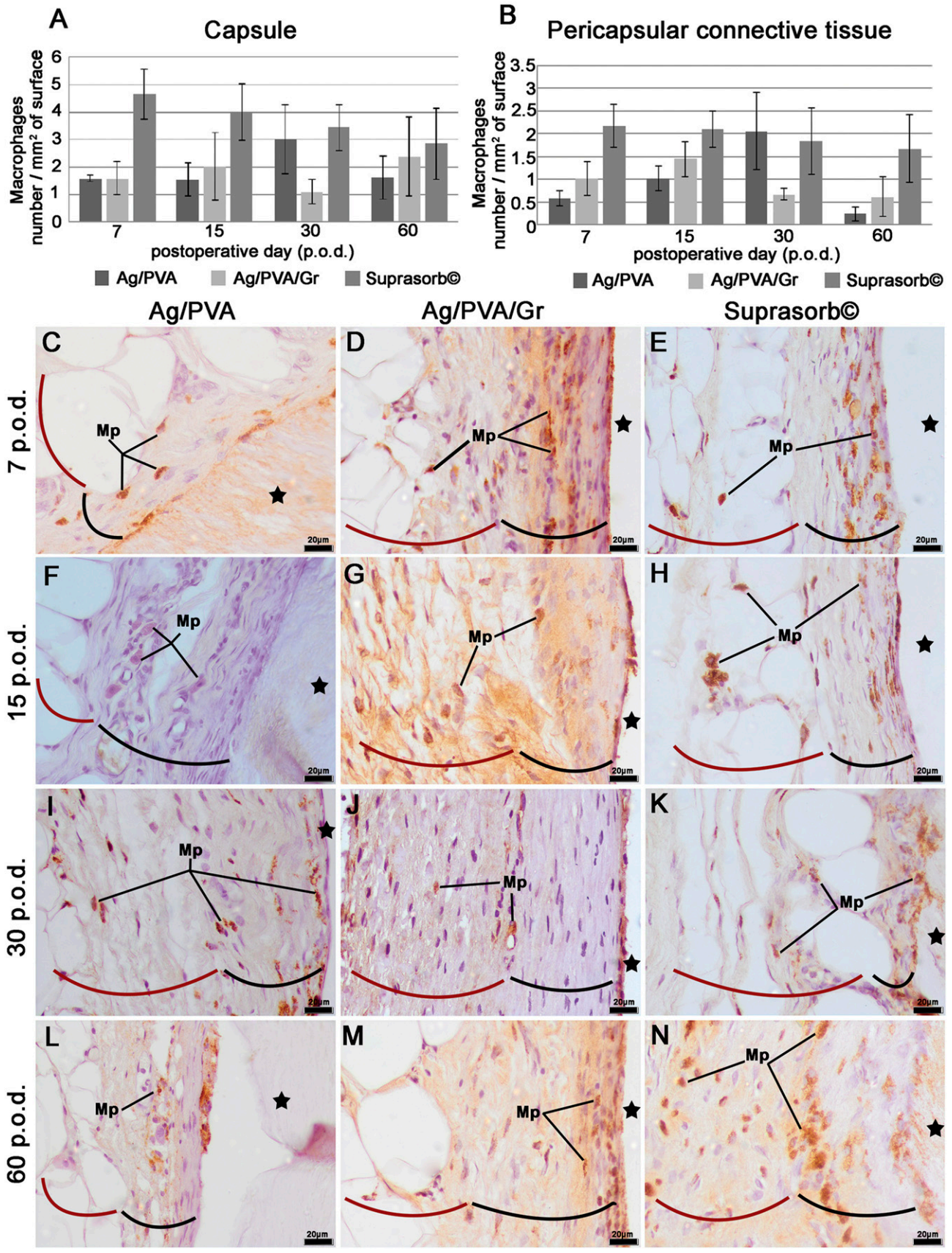

Figure 6. (a, b) CD68^{+} positive macrophages in the connective tissue capsule and pericapsular connective tissue (Mp – macrophages, star – implant location, black curved line – capsule, red curved line - pericapsular connective tissue), Ag/PVA, 7th, 15th, 30th, 60th p.o.d., (c, f, i, l); Ag/PVA/Gr, 7th, 15th, 30th, 60th p.o.d., (d, g, j, m); Suprasorb$^{©}$, 7th, 15th, 30th, 60th p.o.d., (e, h, k, n); bar: 20 µm.

moderate tissue response at the implantation site, considering the gradations in the processing of TIRI.

Many researchers have been particularly interested in studying the foreign body-type reaction characterized by the accumulation of macrophages and giant cells (fused macrophages) on the contact surface between implants and surrounding tissue.[57–60] It is believed that the increased number of macrophages and giant cells is associated with the increase in surface area of more voluminous implants, depending on the size, shape, structure, and binding surface at the point of contact.[61–64] Proper interpretation of the number of macrophages and giant cells in the periimplant zone is especially important today, when nanomaterials that have larger contact surfaces with the surrounding tissue are increasingly used in tissue engineering for scaffold construction.[46,65] In line with this opinion is Ratner's proposal,[7] which presents a new formula for quantitative assessment of biocompatibility, according to which biocompatibility is directly proportional to the number of macrophages, among other criteria.[66] We interpreted the increasing number of macrophages and giant cells in the periimplant zone of the Ag/PVA/Gr material in all monitored time periods (7th, 15th, 30th, and 60th p.o.d.) by using this formula. What we observed is that macrophages appear very early after implantation which is in agreement with the findings of other autors.[7,65,67–69] High numbers of macrophages in the connective tissue around the commercial Suprasorb© were expected, considering the nature of the calcium alginate material which is easily decomposed in the dermis. The structure of polyvinyl hydrogels that contain silver and graphene materials should make a difference in the connective tissue response, so a well-formed capsule, signs of connective collagen production, and infiltration of leukocytes are expected here, according to Ratner's formula for biocompatibility assessment.[7,21,54] Macrophages are present in all observed time periods (7th, 15th, 30th, and 60th p.o.d.) and follow the stages of skin regeneration. Differences in the number of macrophages in the testing periods are in line with expectations of the tissue response. Thus, it is interpreted that the increased number of macrophages in the periimplantation connective tissue around the new Ag/PVA/Gr on the 15th and 30th p.o.d. corresponds to the processes of proper skin recovery in the chronic phase of wound inflammation,[70] where phagocytosis is expected and is a desirable host reaction to a foreign body. The next stage of our research will deal with the classification and quantification of the macrophage phenotype because many authors in recent years have shown the importance of macrophage characterization. That is important in clarifying dilemmas about the different reaction to various implants, which is considered to have a connection with different macrophages behavior that arises as a consequence of other activation mechanisms of M1 and M2 line populations.[71–74]

One of the constant issues that appear around some implants is the inability of macrophages to eliminate inflammation and their tendency to be in a state of so-called frustrated phagocytosis. During the initial phase of inflammation, proinflammatory macrophages (M1-polarized) induce an acute reaction to trauma and foreign material, while tolerogenic anti-inflammatory macrophages (M2-polarized) control the withdrawal of inflammation and induce the next phase which is healing.[67] However, implanted materials can induce a mixed pro and anti-inflammatory phenotype, and thus support the maintenance of chronic inflammation followed by microorganism infection and implantation failure.[68] Therefore, the immunomodulatory properties of implant coating materials in the future should become part of personalized medicine (so-called personalized implant therapies).[66,67] M2 macrophages are involved in the withdrawal of inflammation and wound healing.[66] They secrete TGF-β, PDGF, MMPs, CCL7, and CCL8 which stimulate fibroblast proliferation, migration, and activation and increase collagen synthesis in myofibroblasts, thus promoting fibrosis.[62,69,75] Some authors note that certain factors released from M2 macrophages, such as CCL18 (CC chemokine ligand 18), can sustain chronic inflammation and delay healing.[67–69]

Conclusion

The present study focused on changes in the prevalence of macrophages, as the primary cellular marker of foreign body response in the biocompatibility assessment of various implants. Macrophages were present in both the capsular and pericapsular space, but were more numerous in the capsular area. The numerical density of macrophages in both the capsule and pericapsular connective tissue increased significantly on the 7th and 15th p.o.d. around all observed materials as expected for the chronic phase of the tissue response. Observations on the 30th p.o.d. showed a significant increase in the number of macrophages around Ag/PVA compared to Ag/PVA/Gr. The number of macrophages on the 60th p.o.d. around Ag/PVA declined significantly, but in the area of the novel AG/PVA/Gr it lowered slightly. A striking finding in this period (60th p.o.d.) was the higher abundance of macrophages in the tissue surrounding AG/PVA/Gr compared to Ag/PVA. These differences indicate that in the case of Ag/PVA/Gr a thicker capsule is formed, significantly infiltrated by macrophages and with a larger number of giant cells. Our conclusion is that the addition of graphene to Ag/PVA achieved strong and effective binding to the extracellular matrix elements and affects signaling molecules in the tissue in such a way that stimulates the activation of physical and chemical bonds. As a result, a micro-environment is created which plays a major role in shaping the biological response in a specific way which modulates wound healing, regeneration, and integration of biomaterials into the tissue. When

comparing the tissue response stimulated by the newly synthetized hydrogels with the commercial Suprasorb©, a significant difference is evident. High number of macrophages were detected around and within Suprasorb© in all observed time periods, which suggests that Suprasorb© produces a different micro-environment in the tissue. The physical and chemical properties and the microstructure of Suprasorb© lead to its rapid and intense dissolving and degrading in the tissue, followed by macrophages penetration in the whole area of this biomaterial. The Suprasorb© was intensively phagocytosed by the macrophages, and its short duration in the tissue was confirmed by the low number of giant cells. The biomaterials that persist in the host tissue, as was the case with the observed hydrogels which do are not dissolved and degraded so fast, create a possibility for tissue recovery.

Declaration of conflicting interests

The authors declared no potential conflicts of interest with respect to the research, authorship and/or publication of this article.

Funding

The author(s) disclosed receipt of the following financial support for the research, authorship, and/or publication of this article: The study was supported by the Ministry of Education, Science and Technological Development of the Republic of Serbia (Contract number 451-03-9/2021-14/200143, 451-03-9/2021-14/200135 and 451-03-9/2021-14/200287). The authors also wish to acknowledge the funding from the European Union's Horizon 2020 research and innovation programme under grant agreement No. 952033.

ORCID iD

Danica Markovic https://orcid.org/0000-0002-3403-0473

References

1. Upman PJ and Muench T. Comprehensive scoring system for biomaterial implants, American College of Toxicology Presentation. *Int J Toxicol* 2004; 23: P384.
2. Williams DF. Definitions in biomaterials. Proceedings of a Consensus Conference of the European Society for Biomaterials, Chester, UK, 3–5 March 1986. Amsterdam, the Netherlands: Elsevier, 2004.
3. Geckil H, Xu F, Zhang X, et al. Engineering hydrogels as extracellular matrix mimics. *Nanomedicine* 2010; 5(3): 469–484.
4. Surudžić R, Janković A, Mitrić M, et al. The effect of graphene loading on mechanical, thermal and biological properties of poly(vinyl alcohol)/graphene nanocomposites. *J Ind Eng Chem* 2016; 34: 250–257.
5. Wu JQ, Liu Y, Yang TF, et al. [Porous polyvinyl alcohol hydrogel composite prepared and studied initially for biocompatibility]. *Sichuan da Xue Xue Bao Yi Xue Ban* 2007; 38: 705–724.
6. Zavan B, Cortivo R and Abatangelo G. Hydrogels and tissue engineering. In: Barbucci R (ed) *Hydrogels biological properties and applications*. Italia: Milano; 2009, pp. 1–8.
7. Ratner BD. A pore way to heal and regenerate: 21st century thinking on biocompatibility. *Regen Biomater* 2016; 3: 107–110.
8. Williams FM. In vitro studies-how good are they at replacing in vivo studies for measurement of skin absorption? *Environ Toxicol Pharmacol* 2006; 21: 199–203.
9. Nešović K, Janković A, Radetić T, et al. Chitosan-based hydrogel wound dressings with electrochemically incorporated silver nanoparticles – in vitro study. *Eur Polym J* 2019; 121: 109257.
10. Abudabbus MM, Jevremović I, Janković A, et al. Biological activity of electrochemically synthesized silver doped polyvinyl alcohol/graphene composite hydrogel discs for biomedical applications. *Compos B Eng* 2016; 104: 26–34.
11. LužajićBožinovski T, Marković D, Todorović V, et al. In vivo investigation of soft tissue response of novel silver/poly(vinyl alcohol)/graphene and silver/poly(vinyl alcohol)/chitosan/graphene hydrogels aimed for medical applications–the first experience. *Acta Vet* 2018; 68: 321–339.
12. Nešović K, Abudabbus MM, Rhee KY, et al. Graphene based composite hydrogel for biomedical applications. *Croat Chem Acta* 2017; 90(2): 207–213.
13. Marković D, Kojić Z, Marinković D, et al. Histological and immunohistochemical evaluations of rat soft tissue response to bioceramical implants. *Acta Vet* 2009; 59: 243–253.
14. Stojkovska J, Djurdjevic Z, Jancic I, et al. Comparative in vivo evaluation of novel formulations based on alginate and silver nanoparticles for wound treatments. *J Biomater Appl* 2018; 32(9): 1197–1211.
15. Stojanovic D, Janackovic DJ, Markovic D, et al. A tissue-implant reaction associated with subcutaneous implantation of alpha-tricalcium phosphate, dental ceramic, and hydroxyapatite bioceramics in rats. *Acta Vet* 2008; 58: 381–393.
16. Prokić BB, Lužajić Božinovski T, Gajdov V, et al. Animal models in bicompatibility assessments of implants in soft and hard tissues. *Vet Glasnik* 2021: 1–16, DOI: 10.2298/VETGL210322005P.
17. Anderson JM and Miller KM. Biomaterial biocompatibility and the macrophage. *Biomaterials* 1984; 5: 5–10.
18. Trindade R, Albrektsson T, Tengvall P, et al. Foreign body reaction to biomaterials: on mechanisms for buildup and breakdown of osseointegration. *Clin Implant Dent Relat Res* 2016; 18(1): 192–203.
19. Kamoun EA, Kenawy E-RS and Chen X. A review on polymeric hydrogel membranes for wound dressing applications: PVA-based hydrogel dressings. *J Adv Res* 2017; 8: 217–233.
20. Mir M, Ali MN, Barakullah A, et al. Synthetic polymeric biomaterials for wound healing: a review. *Prog Biomater* 2018; 7: 1–21.
21. Sood A, Granick MS and Tomaselli NL. Wound dressings and comparative effectiveness data. *Adv Wound Care* 2014; 3(8): 511–529.

22. Ratner BD and Atzet S. Hydrogels for healing. In: Barbucci R (ed) *Hydrogels biological properties and applications*. Italia: Milano; 2009, pp. 43–51.
23. Gonzalez JS, Ludueña LN, Ponce A, et al. Poly(vinyl alcohol)/cellulose nanowhiskers nanocomposite hydrogels for potential wound dressings. *Mater Sci Eng C* 2014; 34: 54–61.
24. Abdelgawad AM, Hudson SM and Rojas OJ. Antimicrobial wound dressing nanofiber mats from multicomponent (chitosan/silver-NPs/polyvinyl alcohol) systems. *Carbohydr Polym* 2014; 100: 166–178.
25. Pencheva D, Bryaskova R and Kantardjiev T. Polyvinyl alcohol/silver nanoparticles (PVA/AgNps) as a model for testing the biological activity of hybrid materials with included silver nanoparticles. *Mater Sci Eng C* 2012; 32: 2048–2051.
26. Loo C-Y, Young PM, Lee W-H, et al. Non-cytotoxic silver nanoparticle-polyvinyl alcohol hydrogels with anti-biofilm activity: designed as coatings for endotracheal tube materials. *Biofouling* 2014; 30: 773–788.
27. Li C, Fu R, Yu C, et al. Silver nanoparticle/chitosan oligosaccharide/poly(vinyl alcohol) nanofibers as wound dressings: a preclinical study. *Int J Nanomed* 2013; 8: 4131–4145.
28. Oliviera RN, Rouzé R, Quilty B, et al. Mechanical properties and in vitro characterization of polyvinyl alcohol-nano-silver hydrogel wound dressings. *Int Focus* 2014; 4: 20130049.
29. Chen H, Cheng R, Zhao X, et al. An injectable self-healing coordinative hydrogel with antibacterial and angiogenic properties for diabetic skin wound repair. *NPG Asia Mat* 2019; 11(1): 1–12.
30. Fan Z, Liu B, Wang J, et al. A novel wound dressing based on Ag/graphene polymer hydrogel: effectively kill bacteria and accelerate wound healing. *Adv Funct Mater* 2014; 24: 3933–3943.
31. Nešović K, Janković A, Perić-Grujić A, et al. Kinetic models of swelling and thermal stability of silver/poly(vinyl alcohol)/chitosan/graphene hydrogels. *J Ind Eng Chem* 2019; 77: 83–96.
32. Usman A, Hussain Z, Riaz A, et al. Enhanced mechanical, thermal and antimicrobial properties of poly(vinyl alcohol)/graphene oxide/starch/silver nanocomposites films. *Carbohydr Polym* 2016; 153: 592–599.
33. Hegab HM, Elmekawy A, Zou L, et al. The controversial antibacterial activity of graphene-based materials. *Carbon* 2016; 105: 362–376.
34. Abudabbus MM, Jevremović I, Nešović K, et al. In situ electrochemical synthesis of silver-doped poly(vinyl alcohol)/graphene composite hydrogels and their physicochemical and thermal properties. *Compos B Eng* 2018; 140: 99–107.
35. Williams DF. On the nature of biomaterials. *Biomaterials* 2009; 30: 5897–5909.
36. Ward WK, Slobodzian EP, Tiekotter KL, et al. The effect of microgeometry, implant thickness and polyurethane chemistry on the foreign body response to subcutaneous implants. *Biomaterials* 2002; 23: 4185–4192.
37. Sharma J, Lizu M, Stewart M, et al. Multifunctional nanofibers towards active biomedical therapeutics. *Polymers* 2015; 7: 186–219.
38. Han S, Sun J, He S, et al. The application of graphene-based biomaterials in biomedicine. *Am J Transl Res* 2019; 11(6): 3246–3260.
39. Sheikh Z, Brooks P, Barzilay O, et al. Macrophages, foreign body giant cells and their response to implantable biomaterials. *Materials* 2015; 8: 5671–5701.
40. Luttikhuizen DT, Harmsen MC and Luyn MJAV. Cellular and molecular dynamics in the foreign body reaction. *Tissue Eng* 2006; 12: 1955–1970.
41. Anderson JM, Rodriguez A and Chang DT. Foreign body reaction to biomaterials. *Semin Immunol* 2008; 20: 86–100.
42. Ye Q, Harmsen MC, van Luyn MJA, et al. The relationship between collagen scaffold cross-linking agents and neutrophils in the foreign body reaction. *Biomaterials* 2010; 31: 9192–9201.
43. Dadsetan M, Jones JA, Hiltner A, et al. Surface chemistry mediates adhesive structure, cytoskeletal organization, and fusion of macrophages. *J Biomed Mater Res* 2004; 71A: 439–448.
44. Ikeda T, Ikeda K, Sasaki K, et al. IL-13 as well as IL-4 induces monocytes/macrophages and a monoblastic cell line (UG3) to differentiate into multinucleated giant cells in the presence of M-CSF. *Biochem Biophys Res Commun* 1998; 253: 265–272.
45. Brodbeck WG, Colton E and Anderson JM. Effects of adsorbed heat labile serum proteins and fibrinogen on adhesion and apoptosis of monocytes/macrophages on biomaterials. *J Mater Sci Mater Med* 2003; 14: 671–675.
46. Hench LL and Thompson I. Twenty-first century challenges for biomaterials. *J R Soc Interf* 2010; 7(Suppl 4): S379–S391.
47. Xia Z and Triffitt JT. A review on macrophage responses to biomaterials. *Biomed Mater (Bristol, England)* 2006; 1(1): R1–R9.
48. MacLauchlan S, Skokos EA, Meznarich N, et al. Macrophage fusion, giant cell formation, and the foreign body response require matrix metalloproteinase 9. *J Leukoc Biol* 2009; 85(4): 617–626.
49. Wujcik EK and Monty CN. Nanotechnology for implantable sensors: carbon nanotubes and graphene in medicine. *Wiley Interdiscip Rev Nanomed Nanobiotechnol* 2013; 5: 233–249.
50. Thompson BC, Murray E and Wallace GG. Graphite oxide to graphene. biomaterials to bionics. *Adv Mater* 2015; 27(46): 7563–7582.
51. Ji H, Sun H and Qu X. Antibacterial applications of graphene-based nanomaterials: recent achievements and challenges. *Adv Drug Deliv Rev* 2016; 105: 176–189.
52. Hotaling NA, Tang L, Irvine DJ, et al. Biomaterial strategies for immunomodulation. *Annu Rev Biomed Eng* 2015; 17: 317–349.

53. Sjögren G, Sletten G and Dahl JE. Cytotoxicity of dental alloys, metals, and ceramics assessed by millipore filter, agar overlay, and MTT tests. *J Prosthet Dent* 2000; 84(2): 229–236.
54. Lužajić Božinovski T, Milošević I, Todorović V, et al. Evaluation of soft tissue regenerative process after subcutaneous implantation of silver/poly(vinyl alcohol) and novel silver/poly(vinyl alcohol)/graphene hydrogels in an animal model. *Acta Vet* 2021; 71(3). DOI: 10.2478/acve-2021-0025.
55. Collier TO and Anderson JM. Protein and surface effects on monocyte and macrophage adhesion, maturation, and survival. *J Biomed Mater Res* 2002; 60: 487–496.
56. Ross J, Auger M, Burke B, et al The biology of the macrophage. *Macrophage* 2002; 2: 16–23.
57. DeFife KM, Colton E, Nakayama Y, et al. Spatial regulation and surface chemistry control of monocyte/macrophage adhesion and foreign body giant cell formation by photochemically micropatterned surfaces. *J Biomed Mater Res* 1999; 45: 148–154.
58. Hunt JA and Shoichet M. Biomaterials: surface interactions. *Curr Opin Solid State Mater Sci* 2001; 5: 161–162.
59. Salthouse TN. Some aspects of macrophage behavior at the implant interface. *J Biomed Mater Res* 1984; 18: 395–401.
60. Shanbhag AS, Jacobs JJ, Black J, et al. Macrophage/particle interactions: effect of size, composition and surface area. *J Biomed Mater Res* 1994; 28: 81–90.
61. Kao WJ, Zhao QH, Hiltner A, et al. Theoretical analysis ofin vivo macrophage adhesion and foreign body gaint cell formation on polydimethylsiloxane, low density polyethylene, and polyetherurethanes. *J Biomed Mater Res* 1994; 28: 73–79.
62. Garrigues GE, Cho DR, Rubash HE, et al. Gene expression clustering using self-organizing maps: analysis of the macrophage response to particulate biomaterials. *Biomaterials* 2005; 26: 2933–2945.
63. Shen M and Horbett TA. The effects of surface chemistry and adsorbed proteins on monocyte/macrophage adhesion to chemically modified polystyrene surfaces. *J Biomed Mater Res* 2001; 57: 336–345.
64. Brodbeck WG, MacEwan M, Colton E, et al. Lymphocytes and the foreign body response: lymphocyte enhancement of macrophage adhesion and fusion. *J Biomed Mater Res A* 2005; 74A: 222–229.
65. Anderson JM. Future challenges in thein vitroandin vivoevaluation of biomaterial biocompatibility. *Regen Biomater* 2016; 3(2): 73–77.
66. Martinez FO and Gordon S. The M1 and M2 paradigm of macrophage activation: time for reassessment. *F1000prime Rep* 2014; 6: 13.
67. Gordon S, Plüddemann A and Martinez Estrada F. Macrophage heterogeneity in tissues: phenotypic diversity and functions. *Immunological Rev* 2014; 262: 36–55.
68. Kzhyshkowska J, Gudima A, Riabov V, et al. Macrophage responses to implants: prospects for personalized medicine. *J Leukoc Biol* 2015; 98: 953–962.
69. Ohashi W, Hattori K and Hattori Y. Control of macrophage dynamics as a potential therapeutic approach for clinical disorders involving chronic inflammation. *J Pharmacol Exp Ther* 2015; 354: 240–250.
70. Han G and Ceilley R. Chronic wound healing: a review of current management and treatments. *Adv Ther* 2017; 34(3): 599–610.
71. Bygd HC, Ma L and Bratlie KM. Physicochemical properties of liposomal modifiers that shift macrophage phenotype. *Mater Sci Eng C* 2017; 79: 237–244.
72. Bryant SJ and Peyton SR. Zwitterionic PEG-PC hydrogels modulate the foreign body response in a modulus-dependent manner. *Biomacromolecules* 2018; 19(7): 2880–2888.
73. Li Z and Bratlie KM. How cross-linking mechanisms of methacrylated gellan gum hydrogels alter macrophage phenotype. *ACS Appl Bio Mater* 2019; 2(1): 217–225.
74. Xu Z, Hwang D-G, Bartlett MD, et al. Alter macrophage adhesion and modulate their response on hydrophobically modified hydrogels. *Biochem Eng J* 2021; 165: 107821.
75. Anderson JM, Defife K, McNally A, et al. Monocyte, macrophage and foreign body giant cell interactions with molecularly engineered surfaces. *J Mater Sci Mater Med* 1999; 10: 579–588.